

---

# FedCore: Straggler-Free Federated Learning with Distributed Coresets

---

Hongpeng Guo<sup>1</sup> Haotian Gu<sup>2</sup> Xiaoyang Wang<sup>1</sup> Bo Chen<sup>1</sup>  
 Eun Kyung Lee<sup>3</sup> Tamar Eilam<sup>3</sup> Deming Chen<sup>1</sup> Klara Nahrstedt<sup>1</sup>  
<sup>1</sup>UIUC <sup>2</sup>UC Berkeley <sup>3</sup>IBM Research  
 {hg5, xw28, boc2, dchen, klara}@illinois.edu  
 haotian\_gu@berkeley.edu  
 {eunkyung.lee, eilamt}@us.ibm.com

## Abstract

Federated learning (FL) is a machine learning paradigm that allows multiple clients to collaboratively train a shared model while keeping their data on-premise. However, the straggler issue, due to slow clients, often hinders the efficiency and scalability of FL. This paper presents FedCore, an algorithm that innovatively tackles the straggler problem via the decentralized selection of *coresets*, representative subsets of a dataset. Contrary to existing centralized coreset methods, FedCore creates coresets directly on each client in a distributed manner, ensuring privacy preservation in FL. FedCore translates the coreset optimization problem into a more tractable k-medoids clustering problem and operates distributedly on each client. Theoretical analysis confirms FedCore’s convergence, and practical evaluations demonstrate an **8x** reduction in FL training time, without compromising model accuracy. Our extensive evaluations also show that FedCore generalizes well to existing FL frameworks<sup>1</sup>.

## 1 Introduction

Federated learning (FL) enables multiple clients to collaboratively train a shared machine learning model while retaining their data locally. It has greatly enhanced various privacy-sensitive domains by harnessing the power of AI and providing tailored solutions, including cancer diagnosis [47, 20, 29], urban transportation surveillance [32, 11], financial services [55, 33] and beyond. Federated learning has given rise to several research areas, including model convergence optimization [36, 54, 30], FL system efficiency [24, 25, 14], privacy preservation [38, 3], and robustness against adversarial attacks [34]. Among these areas, the straggler problem, caused by slow or unresponsive clients, hinders overall training efficiency and scalability. Meta’s million-client FL system, Papaya [18], demonstrated that per-client training time distribution spans over two orders of magnitude, and the round completion time is 21x larger than the average training time per client due to stragglers’ delays. Thus, efficient straggler mitigation is vital to unlock FL’s full potential across diverse applications.

**Motivations.** Existing solutions like client selection mechanisms [40, 25, 24] and asynchronous frameworks [54, 39, 18, 52, 31, 7] aim to mitigate the straggler issue in federated learning (FL). However, these methods inherently treat the symptoms rather than the cause. Client selection can result in biased training *data* due to the exclusion of slower clients, while asynchronous approaches can encounter staleness and inconsistency due to laggard updates from stragglers with slow *hardware*. These strategies don’t directly address the root cause of the straggler issue, which is due to the *system and data volume heterogeneity* among clients in FL. The disparities in both computational capacity and data volume lead to varied training times, impacting overall efficiency.

<sup>1</sup>Code: <https://github.com/hongpeng-guo/FedCore>

Instead of sidestepping this fundamental challenge, our approach confronts it directly by *aligning each client’s data volume with its computational capability*. Recognizing that upgrading clients’ hardware is impractical, we propose adjusting the amount of data processed by each slow client. These straggler clients often hold more data than can be efficiently processed within the allotted round time. To address this, we propose creating a representative **coreset**, a compact subset of the full dataset that encapsulates essential learning information. This strategy offers a more precise and direct solution to the straggler problem in FL.

In contrast to existing coreset generation solutions [37, 23], where training data are collected on a central server to create a single coreset, we propose a *distributed* approach that forms training coresets on each client independently, maintaining the *privacy* integral to FL. This task is challenging, particularly when dealing with heterogeneous data distribution across numerous clients, each requiring different coreset sizes based on their computational capabilities. Further complexity arises from the dynamic nature of machine learning models, which is constantly updated during the training process, necessitating the creation of adaptive coresets that can be adjusted according to different model parameters and training phases. To tackle these issues, we designed FedCore which addresses two key **questions**:

- (Q1) How can we select statistically unbiased coresets that adapt to continuously updated models?
- (Q2) How to seamlessly integrate coreset generation with minimal overhead into FL frameworks?

**Methods and Results.** To generate statistically unbiased coresets that adapt to the evolving ML models, we design FedCore, which is applied independently to each client. FedCore operates by periodically searching for a coreset at the start of each FL round, ensuring that the selected coresets may differ between training rounds. This adaptability allows for the provision of the most suitable learning samples, taking into account the varying model parameters at different stages of training (Q1). To minimize coreset generation overhead, we employ gradient-based methods that leverage the per-sample gradients obtained during the gradient descent model training. By repurposing these gradients as input for our coreset algorithm, we optimize the use of available resources and eliminate the need for additional computations. Furthermore, we tackle the intricate coreset optimization problem by transforming it into a more manageable k-medoids clustering problem. This transformation allows for a more efficient resolution of the optimization task, streamlining the overall process and minimizing the system overhead (Q2). Overall, this paper offers the following **contributions**:

- (1) We design and implement the FedCore algorithm, a pioneering solution that leverages distributed coreset training to address the straggler problem in FL with minimal system overhead.
- (2) We provide a theoretical convergence analysis for the FedCore algorithm, which manages to incorporate the coreset gradient approximation error with the federated optimization error, proving that federated model training with per-client coresets results in highly accurate models.
- (3) We extensively evaluate FedCore against existing solutions and baselines. Evaluation results indicate an 8x reduction in FL training time without degrading model accuracy compared to baseline FedAvg. In comparison to FedProx, which handles stragglers through fewer local training epochs, FedCore consistently achieves faster convergence and high model accuracy.

The rest of the paper is organized as follows. We survey related literature in section 2. In section 3, we present the problem setups. In section 4, we present detailed FedCore algorithms and system framework. We provided convergence analysis for FedCore in section 5. Section 6 presents the implementation and evaluations of FedCore system. Finally, section 7 concludes the paper.

## 2 Related Works

**Coreset Methods for Deep Learning.** Coreset methods are effective in reducing computational complexity and memory requirements in deep learning. They are based on selecting a representative subset, or coreset, from the original dataset to retain essential information while significantly reducing data size. Coresets have been successfully applied to tasks like image classification [13, 12, 45], natural language processing [4, 37], and reinforcement learning [8, 17, 5]. Several approaches for efficient coreset creation include: 1) *Geometry Based Clustering* [9, 46, 49], assuming data points in close proximity share similar properties and forming a coreset by removing clustered redundant data points; 2) *Loss Based Sampling* [51, 2, 43], prioritizing training samples based on their contribution

to the error or loss reduction during neural network training and selecting the most important samples to form the coreset; 3) *Decision Boundary Methods* [10, 35], focusing on selecting data points near the decision boundary as the coreset, as they carry more informative content for model training; and 4) *Gradient Matching Solutions* [37, 23, 44], aiming to select a coreset that closely approximates the gradients produced by the full training dataset during deep model training, ensuring minimal gradient differences. In this paper, we adopt gradient matching methods to construct distributed coresets across federated learning clients. By utilizing per-sample gradients produced during model training, coresets can be efficiently computed with minimal overhead.

**Straggler Prevention in Federated Learning.** Stragglers, slow or unresponsive clients in federated learning, can significantly impact training efficiency and model convergence. Various strategies have been proposed to address this challenge, including: 1) *Client Selection* methods [40, 25, 24, 40] mitigate the impact of stragglers by adaptively selecting a subset of clients based on their performance, training speed, or other criteria. However, this approach may introduce bias in heterogeneous settings, as stragglers with unique and important learning samples could be excluded; 2) *Asynchronous FL* techniques [54, 39, 18, 52, 31, 7] eliminate the need for synchronized communication, enabling clients to update local models and communicate with the server independently. Although asynchronous FL can reduce straggler impact, it may suffer from staleness and inconsistency issues affecting the model performance; 3) *Accommodating Partial Work from Stragglers* approaches [28, 27, 53] adjust local epoch numbers or allow clients to perform partial updates. FedProx [28] introduces a proximal term in the optimization process, accommodating partial updates without severely affecting model convergence. In this paper, we propose FedCore, a novel straggler-resilient training method based on partial-work. Unlike most existing works reducing the number of local epochs, FedCore reduces the number of training samples by creating a coreset. This approach enables FedCore to perform more local optimization steps and explore gradients more deeply, resulting in faster convergence speed and better model accuracy.

### 3 Preliminaries

#### 3.1 Federated Learning System Setup

Consider a set of clients,  $U = \{1, 2, \dots, n\}$ . For each client  $u^i$ , we define  $V^i = \{1, 2, \dots, m^i\}$  as the index set of its training samples, where  $m^i$  represents the size of the training set. The  $j$ -th data point in the training set of client  $u^i$  is denoted as  $(x_j^i, y_j^i)$ , with  $j \in V^i$ .  $x_j^i$  and  $y_j^i$  represent the data and label, respectively. In Federated Learning (FL), the primary objective is to minimize an empirical risk function using the training data from each client. Given a loss function  $L$ , a machine learning model  $f$ , and the model parameter space  $\mathcal{W}$ , the FL problem can be formulated as:

$$w_* = \operatorname{argmin}_{w \in \mathcal{W}} \mathcal{L}(w), \text{ where } \mathcal{L}(w) := \sum_{i \in U} p^i \mathcal{L}^i(w), \quad \mathcal{L}^i(w) := \frac{1}{m^i} \sum_{j \in V^i} \mathcal{L}_j^i(w), \quad (1)$$

Here,  $\mathcal{L}_j^i(w) := L(f(w, x_j^i), y_j^i)$  represents the empirical loss for each sample  $(x_j^i, y_j^i)$ , and  $p^i = \frac{m^i}{\sum_{i \in U} m^i}$  is the weight proportional to the training set size. However, privacy concerns prevent a central server from directly accessing the clients' data and solving Eq.(1). As an alternative, FL algorithms require each client to solve a local problem,  $w^{i,*} = \operatorname{argmin}_{w \in \mathcal{W}} \mathcal{L}^i(w)$ , using their data independently. Through iterative communication rounds, the central server aggregates the local models of each client and approximates the solution to Eq.(1).

In FL, clients typically use gradient descent based algorithms like SGD and ADAM for local training.

The objective is to provide an unbiased estimate of the full gradient, denoted as  $\nabla \mathcal{L}^i(w) = \sum_{j \in V^i} \frac{\partial \mathcal{L}_j^i}{\partial w}$ . SGD optimizers calculate model-gradients based on randomly selected mini-batches of training samples through all the training samples in  $V^i$ . This constitutes one *epoch* of training. In conventional FL, each client performs SGD for multiple epochs, i.e.,  $E$  epochs, before sending its gradients to the central server for global model synchronization. This entire process constitutes one *FL round*. The central server then aggregates the received gradients from participating clients and updates the global model. After multiple rounds, i.e.,  $R$  rounds, of training and synchronization, the global model converges to a satisfactory performance.

The heterogeneity of client training data size and computational capabilities leads to considerable variation in per round training times in Federated Learning. To illustrate, let  $c^i$  represent the computational capability of the  $i$ -th client, which can be inferred from their hardware specifications. Here,  $u_i$  takes  $1/c^i$  seconds to train one data sample. Hence, the per-round training time is  $E \frac{m^i}{c^i}$ ,

where  $E$  is the number of epochs per round. Due to the synchronous nature of FL, slower clients can significantly delay the overall training process, resulting in the *straggler problem*.

### 3.2 Distributed Coresets for Federated Learning.

In FedCore, our goal is to address the straggler problem by strategically selecting a small subset  $S^i \subseteq V^i$  of the full training set  $V^i$  for each  $u^i$ . This enables the model to be trained only on the subset  $S^i$  while still approximately converging to the globally optimal solution (i.e., the model parameters that would be obtained if trained on the entire  $V^i$ ).

Inspired by existing works in gradient-based coreset construction [23, 37], the key idea in FedCore is identifying a small subset  $S^i$  with the weighted sum of its elements' gradients closely approximating the full gradient over  $V^i$ . Unlike previous works, our approach generates distributed coresets across all clients  $u^i, i \in U$ , while still providing global model convergence properties.

To further resolve the straggler problem, we impose a training deadline  $\tau$  on every client, ensuring that each  $u^i$  can complete one round of training within  $\tau$  seconds using the coreset  $S^i$ . Consequently,  $c^i \tau$  represents the maximum number of data samples that can be processed by  $u^i$  within a single training round. We specifically formulate the distributed coresets generation problem as follows:

$$(S^{i,*}, \delta^{i,*}) = \operatorname{argmin}_{S^i \subseteq V^i, \delta^i \in \mathbb{R}_+^{|S^i|}} \mathcal{E}^i(w, S^i, \delta^i), \text{ s.t. } |S^i| \leq c^i \tau / E, \forall i \in U. \quad (2)$$

Here  $\mathcal{E}^i(w, S^i, \delta^i) := \left\| \sum_{j \in V^i} \nabla \mathcal{L}_j^i(w) - \sum_{k \in S^i} \delta_k^i \nabla \mathcal{L}_k^i(w) \right\|$  is the 2-normed distance between the full-set gradient and the coreset gradient when the model parameter is  $w$ .  $\delta^i$  is the weight vector of the coreset elements with  $\dim(\delta^i) = |S^i|$ .

Unfortunately, directly solving the aforementioned optimization problem is infeasible due to three main obstacles: **a)** Finding the optimal coreset  $(S^{i,*}, \delta^{i,*})$  is an NP-hard task, due to the combinatorial nature of the problem, even when the per-element gradient,  $\mathcal{L}_j^i$ , can be calculated through SGD training. **b)** Deep machine learning models have high-dimensional model gradients, containing millions of parameters. Solving the above optimization problem with high-dimensional vectors is practically unmanageable. **c)** Eq.(2) needs to be recalculated for every time the model parameter  $w$  gets updated, which further intensifies the computational complexity. In the following sections, we introduce the design of FedCore and illustrate how it effectively addresses these challenges.

## 4 FedCore Algorithm and System

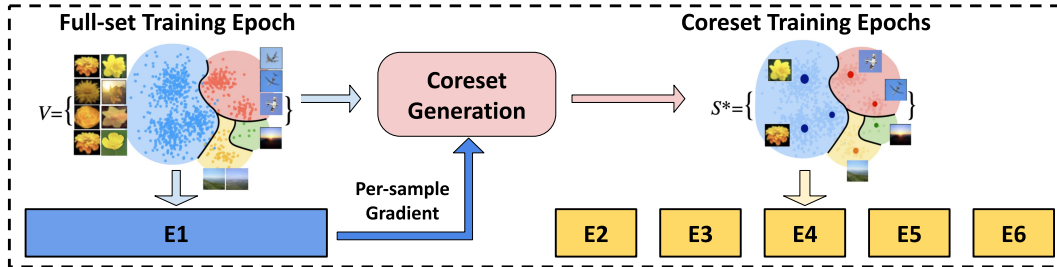


Figure 1: An example workflow of FedCore encompasses a single training round consisting of 6 epochs.

### 4.1 FedCore Algorithm Overview.

We present the FedCore workflow in Algorithm 1. FedCore operates in multiple training rounds, denoted by  $R$ . Like most existing works [28], the server selects  $K$  clients randomly, with probabilities proportional to their training set size, i.e.,  $p^i = \frac{m^i}{\sum_{i \in U} m^i}$  (line 3). The server sends the current model parameter and round deadline  $\tau$  to the selected clients for distributed training (line 4). Clients assess if they can complete full-set training within  $\tau$ . If possible, they execute  $E$  epochs of SGD training over its full-set  $V^i$  (line 7). Otherwise, they generate a training coreset and train using it (line 9 - 11). Finally, clients send their local parameters to the server at the end of each training round, which aggregates them to form a new global model (line 15).

---

**Algorithm 1** FedCore Algorithm
 

---

- 1: **Input:**  $K$ : # selected clients per round.  $R$ : # training rounds.  $w_0$ : # initial model parameter.  
 $E, \tau$ , and  $V^i, c^i, m^i, p^i$  for all  $i \in U$ , as they are defined in section 3.
  - 2: **for**  $r = 0, 1, \dots, R$  **do**
  - 3:   Server randomly selects a subset of  $K$  clients  $U_r$ . Each  $u^i$  is chosen with probability  $p^i$ .
  - 4:   Server sends current model  $w_r$  and round deadline  $\tau$  to all chosen clients  $u^i, i \in U_r$ .
  - 5:   **for each**  $i \in U_r$  **do**
  - 6:     **if**  $E \cdot m^i < c^i \tau$  **then**
  - 7:       Client  $u^i$  executes  $E$  epochs of local training with its full-set  $V^i$ .
  - 8:     **else**
  - 9:       Client  $u^i$  generates approximated gradient distance, either  $\tilde{d}_{j,k}^i$  or  $\hat{d}_{j,k}^i$  for convex models  
       and neural networks, respectively, over the full-set  $V^i$  in the first epoch (section 4.3).
  - 10:      Client  $u^i$  constructs coreset  $(S^{i,*}, \delta^{i,*})$  by solving the k-medoids problem Eq.(5).
  - 11:      Client  $u^i$  executes  $E - 1$  epochs of local training with its coreset  $(S^{i,*}, \delta^{i,*})$ .
  - 12:     **end if**
  - 13:     Client  $u^i$  sends its round-end local parameter  $w_r^i$  back to the server.
  - 14:   **end for**
  - 15:   Server aggregates the new global model:  $w_{r+1} = \frac{1}{K} \sum_{i \in U_r} w_r^i$ .
  - 16: **end for**
- 

To circumvent the need to solve Eq.(2) for every different model parameter  $w$  (i.e., every epoch), we design FedCore to search for a suitable coreset periodically at the beginning of each FL round. Figure 1 illustrates the workflow of FedCore during one FL round. In the first epoch, FedCore processes the entire training set, taking a comprehensive initial optimization step and generating per-sample gradients for coreset creation. For the remaining epochs, FedCore operates on a coreset, significantly reducing training time and mitigating the effects of stragglers.

By minimizing the upper bound of gradient estimation dissimilarity (i.e.,  $\mathcal{E}^i$ ), we transform Eq.(2) into a *k-medoids problem*, which can be solved approximately in polynomial time (section 4.2). We also use low-dimensional gradient approximations as input for the coreset algorithm instead of high-dimensional model gradients, making coreset generation more efficient and lightweight (section 4.3). The distributed coresets generated through our approach provide strong global convergence guarantees (section 5). In the following sections, we detail the design of these algorithms and discuss practical techniques to accelerate FedCore.

## 4.2 Upper Bounding Dissimilarity Estimation with K-Medoids

We aim to construct a coreset  $S^i$  with  $b^i$  elements for each client  $u^i$ . In order to allow for the first epoch of every training round to be full-set with  $m^i$  training elements, we set  $b^i = \lfloor \frac{c^i \tau - m^i}{E-1} \rfloor$  to meet the computational capability  $c^i \tau - m^i$  of  $u^i$  in the remaining  $E - 1$  epochs.

To upper bound the dissimilarity between the full-set gradient and the weighted coreset gradient on  $S^i$ , first consider a mapping function  $\Phi^i : V^i \rightarrow S^i$  that, for every possible model parameter  $w \in \mathcal{W}$ , assigns each data point  $j \in V^i$  to one of its coreset elements  $k \in S^i$ , i.e.,  $\Phi^i(j) = k \in S^i$ . Let  $C_k^i := \{j : \Phi^i(j) = k\} \subseteq V^i$  represent the set of data points assigned to data point  $k \in S^i$ , and let  $\delta_k^i := |C_k^i| \in \mathbb{N}_+$  denote the number of such points. Thus, for any arbitrary  $w \in \mathcal{W}$ , we have

$$\sum_{j \in V^i} \nabla \mathcal{L}_j^i(w) - \sum_{k \in S^i} \delta_k^i \nabla \mathcal{L}_k^i(w) = \sum_{j \in V^i} (\nabla \mathcal{L}_j^i(w) - \nabla \mathcal{L}_{\Phi^i(j)}^i(w))$$

By applying the triangle inequality on both sides, we derive an upper bound for the normed error between the full-set gradient and the weighted coreset gradient, i.e.,

$$\mathcal{E}^i(w, S^i, \delta^i) = \left\| \sum_{j \in V^i} \nabla \mathcal{L}_j^i(w) - \sum_{k \in S^i} \delta_k^i \nabla \mathcal{L}_k^i(w) \right\| \leq \sum_{j \in V^i} \left\| \nabla \mathcal{L}_j^i(w) - \nabla \mathcal{L}_{\Phi^i(j)}^i(w) \right\|. \quad (3)$$

Note that the upper bound in Eq.(3) is minimized when  $\Phi^i$  assigns every data point  $j \in V^i$  to the element  $k \in S^i$  with the most similar gradient, i.e.,  $\Phi^i(j) = \operatorname{argmin}_{k \in S^i} d_{j,k}^i(w)$ , where  $d_{j,k}^i(w) = \left\| \nabla \mathcal{L}_j^i(w) - \nabla \mathcal{L}_k^i(w) \right\|$ . Hence,

$$\min_{S^i \subseteq V^i, \delta^i \in \mathbb{N}_+^{|S^i|}} \mathcal{E}^i(w, S^i, \delta^i) \leq \min_{S^i \subseteq V^i} \left\{ \sum_{j \in V^i} \min_{k \in S^i} d_{j,k}^i(w) \right\}. \quad (4)$$

Recall that the minimum value of Eq.(2) is further upper bounded by the left hand side of Eq.(4), as it has a larger feasible set for its weight vector  $\delta^i \in \mathbb{R}_+^{|S^i|}$ . Hence, we can adjust the optimization objective of Eq.(2) to the right hand side gradient dissimilarity upper bound as follows:

$$(S^{i,*}, \delta^{i,*}) = \operatorname{argmin}_{S^i \subseteq V^i} \left\{ \sum_{j \in V^i} \min_{k \in S^i} d_{j,k}^i(w) \right\}, \quad \text{s.t. } |S^i| \leq b^i, \quad \forall i \in U, \quad (5)$$

where  $\delta^i \in \mathbb{N}_+^{|S^i|}$  is the weight vector associated with  $S^i$ , given by

$$\delta_k^{i,*} = |\{j \in V^i : k = \operatorname{argmin}_{l \in S^{i,*}} d_{j,l}^i(w)\}|.$$

Note that Eq.(5) is a *k-medoids problem* with a budget size of  $b^i$ . The goal is to minimize the objective function by finding the  $b^i$  medoids of the entire training set in the gradient space.

The *k-medoids problem* is a clustering technique forming  $k$  clusters based on data point similarities. K-medoids use actual data points as cluster centers, i.e., the medoids, minimizing dissimilarities between data points and their respective medoids. These medoids form a coreset for our Federated Learning problem. Multiple algorithms [37, 22, 48] have been proposed for this problem, offering diverse computational efficiency and quality trade-offs. In our case, we employ the FasterPAM algorithm, known for its speed and accuracy in identifying optimal medoids, efficiently minimizing our equation Eq.(5). In essence, FasterPAM quickly solves the k-medoids problem, generating coresets for large datasets within one second.

### 4.3 Accelerating Coreset Generation with Gradient Approximation.

Solving the k-medoids problem for each  $w \in \mathcal{W}$ , as illustrated in Eq.(5), requires calculating every pairwise gradient difference for the entire training set (i.e.,  $d_{j,k}^i(w)$ ,  $\forall j, k \in V^i$ ). Nonetheless, directly computing the gradient-distances is computationally costly due to the typically high-dimensional nature of the full model gradient, especially in the case of deep neural networks with millions of parameters. This leads to a computationally burdensome k-medoids clustering process. Following the approach in [37], we tackle this challenge by substituting the full gradient differences with lightweight approximations for two general types of machine learning models as below.

**Convex Machine Learning Models.** We utilize the method from [1] that allows for effective gradient distance approximation in convex machine learning models like linear regression, logistic regression, and regularized SVMs. This method approximates the gradient difference between data points using their Euclidean distance, a principle that uniformly applies across the entirety of the parameter space,  $\mathcal{W}$ . By substituting  $d_{j,k}^i(w)$  with  $\tilde{d}_{j,k}^i(w) = \|x_j^i - x_k^i\|$  in Eq.(5), the coreset problem is reframed into a 2-norm k-medoids clustering within the original data space. This adjustment facilitates coresets formation using pre-calculated pairwise Euclidean distances, eliminating per-round generation and reducing training-time cost.

**Deep Neural Networks.** In deep neural networks, gradient changes primarily reflect the loss function’s gradient relative to the last layer’s input [21]. The normed differences of gradients between data points can be effectively bounded as below:

$$\forall i, j, k, \quad d_{j,k}^i(w) \leq \hat{d}_{j,k}^i(w) = c_1 \cdot \left\| \partial \mathcal{L}_j^i(w) / \partial z_j^i - \partial \mathcal{L}_k^i(w) / \partial z_k^i \right\| + c_2,$$

Here,  $z_j^i$  is the input to the last neural network layer from data point  $x_j^i$ , and  $c_1$  and  $c_2$  are constants. We substitute  $d_{j,k}^i$  with  $\hat{d}_{j,k}^i$  in Eq.(5) for optimization.  $\left\| \partial \mathcal{L}_j^i(w) / \partial z_j^i \right\|$  is attainable from the first epoch of full-set training and requires no extra computation. In FedCore, we derive  $\hat{d}_{j,k}^i$  for all pairs  $j, k \in S^i$  in the first FL epoch, thus alleviating the load of high-dimensional k-medoids clustering.

### 4.4 Discussions of Design Choices.

In designing FedCore, we intentionally set the first epoch to train on the entire dataset, generating (approximated) per-sample gradients for k-medoids coreset generation. However, heavily loaded straggling clients may struggle to complete the initial epoch<sup>2</sup>, i.e.,  $c^i \tau < m^i$ . In such cases, FedCore

<sup>2</sup>Existing solutions like FedProx also fail in extreme cases.

can use faster coreset methods not requiring a full epoch of forward and backward propagation. As explained in section 4.3: **a)** Convex FL models can use static coresets to achieve model convergence and train with pre-computed coresets in any epoch, i.e., calculate coresets with pre-computed  $\tilde{d}_{j,k}^i$ ; **b)** Deep neural networks compute approximated pairwise gradient distance,  $\hat{d}_{j,k}^i$ , which is attainable almost as cheap as calculating the loss (with only one step of gradient calculation for the last layer input), instead of a full epoch of forward and backward propagation. As long as the training deadline allows, FedCore prefers to retain the initial full-set epoch, since it offers a more comprehensive representation of the training status by utilizing the entire dataset and establishing a more accurate, well-informed step in beginning of each round of model training.

## 5 Convergence Analysis

The convergence of FedCore is established for strongly convex functions  $\mathcal{L}$  under mild assumptions. It is important to note that most existing works on the convergence analysis of federated learning (e.g., [15, 28, 30]) assume that local gradient estimations at the client level are unbiased since the data is directly sampled from the full-set. However, in FedCore, gradients computed from coresets are biased approximations to full-set gradients. As a result, the main technical contribution of our convergence analysis is to meticulously incorporate the coreset gradient approximation error with the federated optimization error.

**Theorem 5.1** *Assume that for any  $i \in U$ , the loss function  $\mathcal{L}^i$  is  $L$ -smooth and  $\mu$ -strongly convex, and the coreset  $(S^{i,*}, \delta^{i,*})$  constructed in FedCore is an  $\epsilon$ -approximation to the full-set, i.e.*

$$\forall w \in \mathcal{W}, \quad \frac{1}{m^i} \left\| \sum_{j \in V^i} \nabla \mathcal{L}_j^i(w) - \sum_{k \in S^{i,*}} \delta_k^{i,*} \nabla \mathcal{L}_k^i(w) \right\| \leq \epsilon, \quad (6)$$

Consider FedCore with  $R$  rounds with each round containing  $E$  epochs. Set the learning rate  $\eta_t = \Omega(1/t)$  for  $t \in \{1, 2, \dots, ER\}$ . The model  $w_{out}$  output by FedCore after  $R$  rounds satisfies

$$\mathbb{E} [\mathcal{L}(w_{out}) - \mathcal{L}(w_*)] \leq \mathcal{O}(\epsilon) + \mathcal{O}(1/R),$$

where  $w_* = \operatorname{argmin}_{w \in \mathcal{W}} \mathcal{L}(w)$  is the global optimum of  $\mathcal{L}$  in Eq.(1), and the expectation is taken over the randomness in client selection, coreset construction and model initialization.

The comprehensive collections of the technical assumptions and the detailed statement of Theorem 5.1 can be found in appendix A.2 and appendix A.3. The bound in Theorem 5.1 indicates that FedCore converges to the global optimum at the rate  $\mathcal{O}(1/R)$ , with an additional cost of  $\mathcal{O}(\epsilon)$  attributed to the coreset gradient approximation error. It is worth noting that the rate  $\mathcal{O}(1/R)$  aligns with the existing convergence results for federated learning [15, 28, 30]. The trade-off between full-set FL and coreset FL is explicitly characterized in Theorem 5.1. While learning on the full-set may circumvent the gradient approximation error, the straggler problem in full-set FL can lead to a small number of training rounds  $R$  under a limited time budget. On the other hand, FedCore reduces the impact of the straggler problem and allows for more training rounds to achieve a smaller optimization error  $\mathcal{O}(1/R)$ , while keeping the gradient approximation error low (only  $\mathcal{O}(\epsilon)$ ), enabling both efficient and accurate optimization. The proof of Theorem 5.1 is deferred to appendix A.3.

## 6 Evaluations

### 6.1 Experimental Setups

Dataset	Clients	Samples	Samples / Client	
			mean	std
MNIST	1,000	69,035	69	106
Shakespeare	143	517,106	3,616	6,808
Synthetic	30	20,101	670	1,148

**Table 1:** Statistics of the benchmarks

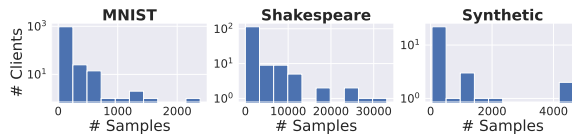


**Figure 2:** Distribution of training samples per client

**FL Datasets and Benchmarks** We assess FedCore using three widely recognized federated learning benchmarks from computer vision, natural language processing, and feature-based classification

domains. These tasks encompass major machine learning model types, including CNN, RNN, and Logistic Regression (LR), as detailed below: **1) MNIST Dataset** [26]: This dataset features a digit classification task using a three-layer CNN for training. To create statistical heterogeneity, the data is allocated among 1,000 clients, where each client has samples of just two distinct digits. The quantity of samples per client adheres to a power-law distribution, highlighting the diversity among clients. **2) Shakespeare Dataset** [36]: This dataset represents a next-character prediction task trained on *the Complete Works of William Shakespeare* using an LSTM model. Each of the 143 speaking roles in the plays is associated with a distinct client. And **3) Synthetic Dataset** [28]: This dataset involves a feature-based classification task with 30 clients training an LR model. Each client’s training data is generated from a random function  $G(\alpha, \beta)$ , where  $\alpha$  and  $\beta$  control the cross-client and within-client data heterogeneity. Following the approach in [28], we evaluate our method with three different parameter settings:  $(\alpha, \beta)$  equals to  $(0, 0)$ ,  $(0.5, 0.5)$  and  $(1, 1)$ , respectively. In our evaluation, we train MNIST, Shakespeare and Synthetic benchmarks for 100, 30 and 100 rounds, respectively. For all three tasks, each round comprises 10 local epochs. Detailed statistics for these three datasets can be found in Table 1 and Figure 2.

**Comparison Baselines** We compare FedCore with the following three baselines.

- a) FedAvg [36] updates the global model by averaging local model updates from participating clients. However, it does not consider training deadlines, and thus, is prone to the stragglers issue.
- b) FedAvg-DS [36] is a variant of FedAvg enforces training deadlines for each round by excluding stragglers. This strategy, however, may negatively impact its overall training performance.
- c) FedProx [28] is designed to handle partial results from stragglers that might complete fewer local epochs than anticipated, FedProx incorporates a quadratic proximal term that explicitly limits the magnitude of local model updates to accommodate stragglers.

**Implementations** We develop FedCore along with all the baseline algorithms using PyTorch [42], extending the simulation framework proposed in FedML[16]. For each client  $u^i$ , we sample its computational capability from a normal distribution, i.e.,  $c^i \sim \mathcal{N}(1, 0.25)$ . As discussed in section 3, the per-round training time for a client is proportional to  $\frac{m^i}{c^i}$ . To emulate the stragglers problem, we designate the slowest  $s\%$  of clients as stragglers by setting a per-round training deadline that these clients cannot complete all their training tasks within the allotted time. When the training deadline is reached, FedAvg-DS simply excludes all stragglers and aggregates a global model using the non-stragglers’ gradients. In contrast, FedProx and FedCore employ different strategies such as reducing local training epochs or training with coresets. In our evaluation, we consider two different stragglers’ settings by choosing  $s$  to be 10 and 30, respectively. A more detailed implementation and hyper-parameters for the evaluation are presented in appendix B.

## 6.2 Evaluation Results

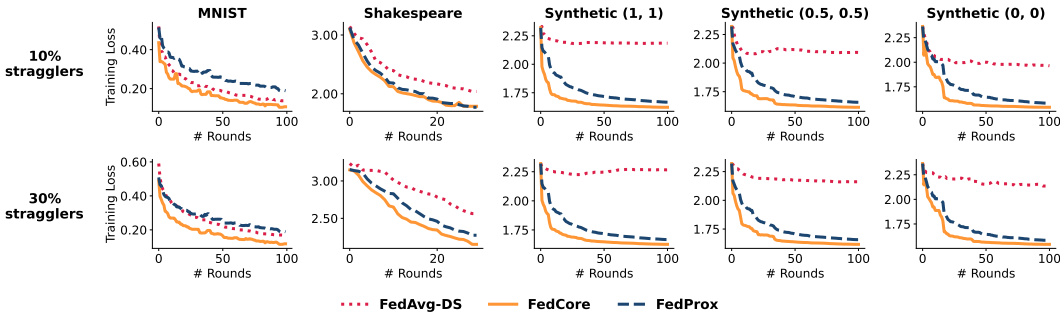


**Figure 3:** The training loss curves for FedAvg-DS, FedCore, and FedProx at 10% and 30% stragglers.

**Model Performance** We present the training loss curves in Figure 3 and model accuracy, along with normalized training time, in Table 2. More evaluation results are depicted in appendix B. For model training loss, FedCore consistently achieves the fastest convergence speed and yields the lowest model loss. In contrast, FedAvg-DS struggles to converge well under synthetic benchmarks



		MNIST		Shakespeare		Synthetic (1, 1)		Synthetic (0.5, 0.5)		Synthetic (0, 0)	
		10%	30%	10%	30%	10%	30%	10%	30%	10%	30%
Test Accuracy	FedAvg	94.7		44.9		71.8		73.7		88.2	
	FedAvg-DS	94.1	93.1	39.0	25.2	23.0	19.9	32.2	23.6	36.3	34.6
	FedProx	92.6	92.7	44.1	31.3	<b>72.3</b>	72.2	74.1	74.1	87.2	87.2
	<b>FedCore</b>	<b>94.6</b>	<b>94.5</b>	<b>44.7</b>	<b>34.8</b>	72.2	<b>72.8</b>	<b>75.2</b>	<b>75.1</b>	<b>88.5</b>	<b>88.3</b>
		<b>3.27</b>	<b>8.48</b>	<b>1.38</b>	<b>4.09</b>	<b>1.37</b>	<b>4.80</b>	<b>1.37</b>	<b>4.80</b>	<b>1.37</b>	<b>4.80</b>
Mean Training Time per Round (normalized)	FedAvg										
	FedAvg-DS	0.94	0.95	0.60	0.67	0.69	0.79	0.69	0.79	0.69	0.79
	FedProx	0.98	0.99	0.85	0.94	0.86	0.95	0.86	0.95	0.86	0.95
	<b>FedCore</b>	0.99	0.99	0.90	0.99	0.93	0.99	0.93	0.99	0.93	0.99

**Table 2:** Comparison of test accuracy and training time for FedAvg, FedAvg-DS, FedProx, and FedCore at 10% and 30% stragglers. **Bold:** top accuracy; **Red:** exceeded deadline. Normalized time of 1 is round deadline.

due to its approach of dropping stragglers, which contain unique training samples essential for learning. FedProx presents competitive performance, but with slower convergence and higher loss compared to FedCore. Concerning test accuracy, FedCore consistently achieves the highest or near-highest values across all datasets and stragglers’ settings, highlighting its superior performance in maintaining or improving model accuracy even with stragglers. FedProx also demonstrates competitive performance, owing to its ability to accommodate partial results from stragglers, which contain a significant amount of unique training samples that improve model accuracy. However, FedAvg-DS often results in lower accuracy, particularly in the 30% stragglers setting, as its approach of dropping straggler clients negatively impacts training performance. In terms of training time, FedCore, FedProx, and FedAvg-DS are deadline-aware, ensuring they do not exceed the round deadlines. While FedCore does not always achieve the fastest training time, it strikes a balance between efficiency and maintaining high accuracy. Conversely, FedAvg exhibits the longest training times, indicated in red, showcasing its vulnerability to stragglers and lack of deadline-awareness.

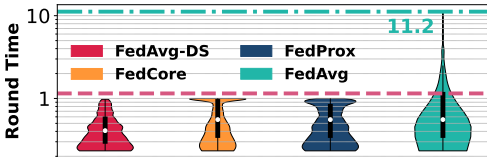


**Figure 4:** Round length distribution on MNIST benchmark, 30% stragglers. The y-axis is presented in log-scale for better illustration.

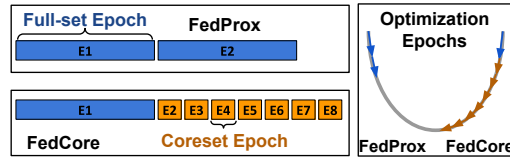


**Figure 5:** Faster FedCore convergence vs. FedProx, due to more coreset-based gradient steps compared to FedProx’s fewer epochs of full-set training.

**Stragglers Handling** Figure 4 presents the distribution of clients’ round times for the MNIST benchmark with 30% stragglers. As the figure illustrates, FedAvg, which is oblivious to round deadlines, generates a tail distribution that can exceed 11 times the allotted training time for a round. In contrast, deadline-aware algorithms like FedCore, FedAvg-DS, and FedProx consistently ensure that each training round is completed before the deadline. Interestingly, the FedCore distribution is more tightly clustered around the round deadline in comparison to FedAvg-DS and FedProx, which signifies a more effective utilization of the allotted training time to accurately follow the gradient direction. Table 2 shows that although FedCore requires slightly longer time than the other two deadline-aware algorithms, it successfully meets the deadline requirements and ultimately achieves the best model performance.

As depicted in Figure 5, FedCore takes advantage of coresets to perform more epochs of local optimization and deeper gradient exploration, as opposed to FedProx’s fewer epochs of full-set training. This approach leads to a faster convergence rate and improved model accuracy, demonstrating the effectiveness of the FedCore algorithm in addressing the straggler problem in federated learning.

## 7 Concluding Remarks

In this paper, we introduce FedCore, an innovative algorithm addressing the straggler problem in federated learning using distributed coresets. FedCore effectively adapts to updated models and integrates coreset generation with minimal overhead, significantly outperforming traditional methods. Our comprehensive analysis and evaluation demonstrate that FedCore substantially reduces FL training time while maintaining high accuracy. With regards to **broader impacts**, this research

pioneers the use of coresets methods in efficient federated learning, paving the way for more scalable and robust systems, especially in privacy-sensitive domains where data protection is vital.

## References

- [1] Zeyuan Allen-Zhu. Katyusha: The first direct acceleration of stochastic gradient methods. In *Proceedings of the 49th Annual ACM SIGACT Symposium on Theory of Computing*, pages 1200–1205, 2017.
- [2] Olivier Bachem, Mario Lucic, and Andreas Krause. Coresets for nonparametric estimation—the case of dp-means. In *International Conference on Machine Learning*, pages 209–217. PMLR, 2015.
- [3] Abhishek Bhowmick, John Duchi, Julien Freudiger, Gaurav Kapoor, and Ryan Rogers. Protection against reconstruction and its applications in private federated learning. *arXiv preprint arXiv:1812.00984*, 2018.
- [4] Jeff Bilmes. Submodularity in machine learning and artificial intelligence. *arXiv preprint arXiv:2202.00132*, 2022.
- [5] Hamid Bostani, Mansour Sheikhan, and Behrad Mahboobi. A strong coreset algorithm to accelerate opf as a graph-based machine learning in large-scale problems. *Information Sciences*, 555:424–441, 2021.
- [6] Stephen Boyd, Stephen P Boyd, and Lieven Vandenbergh. *Convex Optimization*. Cambridge university press, 2004.
- [7] Zheng Chai, Yujing Chen, Ali Anwar, Liang Zhao, Yue Cheng, and Huzefa Rangwala. Fedat: a high-performance and communication-efficient federated learning system with asynchronous tiers. In *Proceedings of the International Conference for High Performance Computing, Networking, Storage and Analysis*, pages 1–16, 2021.
- [8] Souradip Chakraborty, Amrit Singh Bedi, Alec Koppel, Brian M Sadler, Furong Huang, Pratap Tokekar, and Dinesh Manocha. Posterior coreset construction with kernelized stein discrepancy for model-based reinforcement learning. *arXiv preprint arXiv:2206.01162*, 2022.
- [9] Yutian Chen, Max Welling, and Alex Smola. Super-samples from kernel herding. In *Proceedings of the Twenty-Sixth Conference on Uncertainty in Artificial Intelligence*, UAI’10, 2010.
- [10] Melanie Ducoffe and Frederic Precioso. Adversarial active learning for deep networks: a margin based approach. *arXiv preprint arXiv:1802.09841*, 2018.
- [11] Jie Feng, Can Rong, Funing Sun, Diansheng Guo, and Yong Li. Pmf: A privacy-preserving human mobility prediction framework via federated learning. *Proceedings of the ACM on Interactive, Mobile, Wearable and Ubiquitous Technologies*, 2020.
- [12] Sumyung Gang, Ndayishimiye Fabrice, Daewon Chung, and Joonjae Lee. Character recognition of components mounted on printed circuit board using deep learning. *Sensors*, 2021.
- [13] Chengcheng Guo, Bo Zhao, and Yanbing Bai. Deepcore: A comprehensive library for coreset selection in deep learning. In *Database and Expert Systems Applications: 33rd International Conference, DEXA 2022, Vienna, Austria, August 22–24, 2022, Proceedings, Part I*, pages 181–195. Springer, 2022.
- [14] Hongpeng Guo, Haotian Gu, Zhe Yang, Xiaoyang Wang, Eun Kyung Lee, Nandhini Chandramoorthy, Tamar Eilam, Deming Chen, and Klara Nahrstedt. Bofl: bayesian optimized local training pace control for energy efficient federated learning. In *Proceedings of the 23rd ACM/IFIP International Middleware Conference*, pages 188–201, 2022.
- [15] Farzin Haddadpour and Mehrdad Mahdavi. On the convergence of local descent methods in federated learning. *arXiv preprint arXiv:1910.14425*, 2019.
- [16] Chaoyang He, Songze Li, Jinhyun So, Xiao Zeng, Mi Zhang, Hongyi Wang, Xiaoyang Wang, Praneeth Vepakomma, Abhishek Singh, Hang Qiu, et al. Fedml: A research library and benchmark for federated machine learning. *arXiv preprint arXiv:2007.13518*, 2020.
- [17] Yizhou Huang, Kevin Xie, Homanga Bharadhwaj, and Florian Shkurti. Continual model-based reinforcement learning with hypernetworks. In *2021 IEEE International Conference on Robotics and Automation (ICRA)*, pages 799–805. IEEE, 2021.
- [18] Dzmitry Huba, John Nguyen, Kshitiz Malik, Ruiyu Zhu, Mike Rabbat, Ashkan Yousefpour, Carole-Jean Wu, Hongyuan Zhan, Pavel Ustinov, Harish Srinivas, et al. Papaya: Practical, private, and scalable federated learning. *Proceedings of Machine Learning and Systems*, 4:814–832, 2022.

- [19] Intel. Intel core x series core i9 10920x cpu specifications. Online, 2023. URL <https://www.intel.com/content/www/us/en/products/sku/198012/intel-core-i910920x-xseries-processor-19-25m-cache-3-50-ghz/specifications.html>.
- [20] Amelia Jiménez-Sánchez, Mickael Tardy, Miguel A González Ballester, Diana Mateus, and Gemma Piella. Memory-aware curriculum federated learning for breast cancer classification. *arXiv preprint arXiv:2107.02504*, 2021.
- [21] Angelos Katharopoulos and François Fleuret. Not all samples are created equal: Deep learning with importance sampling. In *International Conference on Machine Learning*, pages 2525–2534. PMLR, 2018.
- [22] Leonard Kaufman and Peter J Rousseeuw. *Finding Groups in Data: An Introduction to Cluster Analysis*. John Wiley & Sons, 2009.
- [23] Krishnateja Killamsetty, Sivasubramanian Durga, Ganesh Ramakrishnan, Abir De, and Rishabh Iyer. Gradmatch: Gradient matching based data subset selection for efficient deep model training. In *International Conference on Machine Learning*, pages 5464–5474. PMLR, 2021.
- [24] Young Geun Kim and Carole-Jean Wu. Autofl: Enabling heterogeneity-aware energy efficient federated learning. In *MICRO-54: 54th Annual IEEE/ACM International Symposium on Microarchitecture*, pages 183–198, 2021.
- [25] Fan Lai, Xiangfeng Zhu, Harsha V Madhyastha, and Mosharaf Chowdhury. Oort: Efficient federated learning via guided participant selection. In *Operating Systems Design and Implementation*, pages 19–35, 2021.
- [26] Yann LeCun, Corinna Cortes, and Christopher J. C. Burges. Mnist handwritten digit database. <http://yann.lecun.com/exdb/mnist>, 2010.
- [27] Tian Li, Anit Kumar Sahu, Manzil Zaheer, Maziar Sanjabi, Ameet Talwalkar, and Virginia Smithy. Feddane: A federated newton-type method. In *2019 53rd Asilomar Conference on Signals, Systems, and Computers*, pages 1227–1231. IEEE, 2019.
- [28] Tian Li, Anit Kumar Sahu, Manzil Zaheer, Maziar Sanjabi, Ameet Talwalkar, and Virginia Smith. Federated optimization in heterogeneous networks. *Proceedings of Machine Learning and Systems*, 2:429–450, 2020.
- [29] Wenqi Li, Fausto Milletari, Daguang Xu, Nicola Rieke, Jonny Hancox, Wentao Zhu, Maximilian Baust, Yan Cheng, Sébastien Ourselin, M Jorge Cardoso, et al. Privacy-preserving federated brain tumour segmentation. In *Machine Learning in Medical Imaging: 10th International Workshop*, pages 133–141. Springer, 2019.
- [30] Xiang Li, Kaixuan Huang, Wenhao Yang, Shusen Wang, and Zhihua Zhang. On the convergence of FedAvg on non-iid data. In *International Conference on Learning Representations*, 2020.
- [31] Xingyu Li, Zhe Qu, Bo Tang, and Zhuo Lu. Stragglers are not disaster: A hybrid federated learning algorithm with delayed gradients. *arXiv preprint arXiv:2102.06329*, 2021.
- [32] Yi Liu, JQ James, Jiawen Kang, Dusit Niyato, and Shuyu Zhang. Privacy-preserving traffic flow prediction: A federated learning approach. *IEEE Internet of Things Journal*, 2020.
- [33] Guodong Long, Yue Tan, Jing Jiang, and Chengqi Zhang. Federated learning for open banking. In *Federated Learning: Privacy and Incentive*, pages 240–254. Springer, 2020.
- [34] Lingjuan Lyu, Han Yu, Xingjun Ma, Chen Chen, Lichao Sun, Jun Zhao, Qiang Yang, and S Yu Philip. Privacy and robustness in federated learning: Attacks and defenses. *IEEE Transactions on Neural Networks and Learning Systems*, 2022.
- [35] Katerina Margatina, Giorgos Vernikos, Loïc Barrault, and Nikolaos Aletras. Active learning by acquiring contrastive examples. *arXiv preprint arXiv:2109.03764*, 2021.
- [36] Brendan McMahan, Eider Moore, Daniel Ramage, Seth Hampson, and Blaise Aguera y Arcas. Communication-efficient learning of deep networks from decentralized data. In *Artificial Intelligence and Statistics*, pages 1273–1282. PMLR, 2017.
- [37] Baharan Mirzasoleiman, Jeff Bilmes, and Jure Leskovec. Coresets for data-efficient training of machine learning models. In *International Conference on Machine Learning*, pages 6950–6960. PMLR, 2020.

- [38] Milad Nasr, Reza Shokri, and Amir Houmansadr. Comprehensive privacy analysis of deep learning: Passive and active white-box inference attacks against centralized and federated learning. In *2019 IEEE Symposium on Security and Privacy (SP)*, pages 739–753. IEEE, 2019.
- [39] John Nguyen, Kshitiz Malik, Hongyuan Zhan, Ashkan Yousefpour, Mike Rabbat, Mani Malek, and Dzmitry Huba. Federated learning with buffered asynchronous aggregation. In *International Conference on Artificial Intelligence and Statistics*, pages 3581–3607. PMLR, 2022.
- [40] Takayuki Nishio and Ryo Yonetani. Client selection for federated learning with heterogeneous resources in mobile edge. In *ICC 2019-2019 IEEE International Conference on Communications (ICC)*, pages 1–7. IEEE, 2019.
- [41] NVIDIA. Geforce rtx 2080 ti gpu specifications. Online, 2023. URL <https://www.nvidia.com/en-us/geforce/20-series/>.
- [42] Adam Paszke, Sam Gross, Francisco Massa, Adam Lerer, James Bradbury, Gregory Chanan, Trevor Killeen, Zeming Lin, Natalia Gimelshein, Luca Antiga, Alban Desmaison, Andreas Kopf, Edward Yang, Zachary DeVito, Martin Raison, Alykhan Tejani, Sasank Chilamkurthy, Benoit Steiner, Lu Fang, Junjie Bai, and Soumith Chintala. Pytorch: An imperative style, high-performance deep learning library. In *Advances in Neural Information Processing Systems*, volume 32, pages 8024–8035, 2019.
- [43] Mansheej Paul, Surya Ganguli, and Gintare Karolina Dziugaite. Deep learning on a data diet: Finding important examples early in training. In *Advances in Neural Information Processing Systems*, volume 34, pages 20596–20607, 2021.
- [44] Omead Pooladzandi, David Davini, and Baharan Mirzasoleiman. Adaptive second order coresets for data-efficient machine learning. In *International Conference on Machine Learning*, pages 17848–17869. PMLR, 2022.
- [45] Ozan Sener and Silvio Savarese. Active learning for convolutional neural networks: A core-set approach. *arXiv preprint arXiv:1708.00489*, 2017.
- [46] Ozan Sener and Silvio Savarese. Active learning for convolutional neural networks: A coresets approach. In *International Conference on Learning Representations*, 2018.
- [47] Micah J Sheller, G Anthony Reina, Brandon Edwards, Jason Martin, and Spyridon Bakas. Multi-institutional deep learning modeling without sharing patient data: A feasibility study on brain tumor segmentation. In *Brainlesion: Glioma, Multiple Sclerosis, Stroke and Traumatic Brain Injuries: 4th International Workshop*, pages 92–104. Springer, 2019.
- [48] Weiguo Sheng and Xiaohui Liu. A genetic k-medoids clustering algorithm. *Journal of Heuristics*, 12: 447–466, 2006.
- [49] Christian Sohler and David P Woodruff. Strong coresets for k-median and subspace approximation: Goodbye dimension. In *2018 IEEE 59th Annual Symposium on Foundations of Computer Science (FOCS)*, pages 802–813. IEEE, 2018.
- [50] Sebastian U Stich. Local sgd converges fast and communicates little. In *International Conference on Learning Representations*, 2019.
- [51] Mariya Toneva, Alessandro Sordoni, Remi Tachet des Combes, Adam Trischler, Yoshua Bengio, and Geoffrey J Gordon. An empirical study of example forgetting during deep neural network learning. *arXiv preprint arXiv:1812.05159*, 2018.
- [52] Marten van Dijk, Nhuong V Nguyen, Toan N Nguyen, Lam M Nguyen, Quoc Tran-Dinh, and Phuong Ha Nguyen. Asynchronous federated learning with reduced number of rounds and with differential privacy from less aggregated gaussian noise. *arXiv preprint arXiv:2007.09208*, 2020.
- [53] Jianyu Wang, Qinghua Liu, Hao Liang, Gauri Joshi, and H Vincent Poor. Tackling the objective inconsistency problem in heterogeneous federated optimization. In *Advances in Neural Information Processing Systems*, volume 33, pages 7611–7623, 2020.
- [54] Cong Xie, Sanmi Koyejo, and Indranil Gupta. Asynchronous federated optimization. *arXiv preprint arXiv:1903.03934*, 2019.
- [55] Runhua Xu, Nathalie Baracaldo, Yi Zhou, Ali Anwar, and Heiko Ludwig. Hybridalpha: An efficient approach for privacy-preserving federated learning. In *Proceedings of the 12th ACM Workshop on Artificial Intelligence and Security*, pages 13–23, 2019.

## A Convergence Analysis Proof

### A.1 Problem Settings and Notations

**Problem Set-up** First recall the notations defined in section 3. The federated learning problem is to solve

$$w_* = \operatorname{argmin}_{w \in \mathcal{W}} \mathcal{L}(w), \quad \text{where } \mathcal{L}(w) := \sum_{i \in U} p^i \mathcal{L}^i(w), \quad \mathcal{L}^i(w) := \frac{1}{m^i} \sum_{j \in V^i} \mathcal{L}_j^i(w). \quad (7)$$

with  $\mathcal{L}_j^i(w) := L(f(w, x_j^i), y_j^i)$  representing the empirical loss for each sample  $(x_j^i, y_j^i)$  from the  $i$ -th client, under the model  $f(w, \cdot)$ . Here  $|U| = n$  is the total number of clients, and  $p^i$  is the weight of the  $i$ -th client, proportional to the size  $m^i$  of its training set with  $\sum_{i=1}^n p^i = 1$ .

The proposed federated learning algorithm FedCore consists of  $R$  rounds, each of which contains  $E$  epochs. We use the time index  $t \in \{0, 1, 2, \dots, ER\}$  to denote the time step of each epoch, where  $t = 0$  corresponds to the model initialization. Meanwhile, denote  $w_t^i$  to be the model parameter of client  $i$  at time step  $t$ . One typical round in FedCore is described as follows.

Let  $t = (r - 1)E$  be the beginning at the  $r$ -th round for some  $r = 1, 2, \dots, R$ . The central server broadcasts the latest model,  $w_t$ , to all the devices:

$$w_t^i \leftarrow w_t, \quad \forall i \in U.$$

After that, the central server selects a set  $U_t$  of  $K$  clients randomly from  $U$ , according to the sampling probabilities  $p^i, i \in U$ . The coreset is then constructed for each client  $(S^{i,*}, \delta^{i,*}), i \in U_t$ . Each client  $i \in U_t$  performs local updates on its model  $w_t^i$  for the remaining epochs in the current round, based on the data in its coreset  $(S^{i,*}, \delta^{i,*})$ :

$$w_{t+k+1}^i \leftarrow w_{t+k}^i - \eta_{t+k} g_{t+k}^i, \quad \text{for } k = 0, 1, \dots, E - 1, \quad (8)$$

where  $\eta_{t+k}$  is the learning rate and  $g_{t+k}^i$  is the gradient computed from  $(S^{i,*}, \delta^{i,*})$ :

$$g_{t+k}^i = \frac{1}{m^i} \sum_{j \in S^{i,*}} \delta_j^{i,*} \nabla \mathcal{L}_j^i(w_{t+k}^i). \quad (9)$$

Finally, at the end of the  $r$ -th round, the server aggregates the local models  $\{w_{t+E}^i\}_{i \in U_t}$  to produce the new global model  $w_{t+E}$ :

$$w_{t+E} \leftarrow \frac{1}{K} \sum_{i \in U_t} w_{t+E}^i. \quad (10)$$

Note that the current update in Eq.(8) is written in the form of gradient descent (GD), meaning that the model will be updated once based on the full gradient computed from  $(S^{i,*}, \delta^{i,*})$ . In practice, however, within one epoch, the update in Eq.(8) is usually conducted sequentially using stochastic gradient descent (SGD): the entire coreset will be randomly split into several mini-batches, and the parameter will be updated on each mini-batch. In the following analysis, we focus on the gradient descent setting in Eq.(8) for the ease of presentation. Convergence guarantees for SGD updates can be established by using the similar arguments as in the proofs of our main results.

**Notations** In subsequent analysis, we use

$$G_t^i := \nabla \mathcal{L}^i(w_t^i) = \frac{1}{m^i} \sum_{j \in V^i} \nabla \mathcal{L}_j^i(w_t^i) \quad (11)$$

to denote the full gradient from the full-set  $V^i$  of client  $i$  at time  $t$ . And denote

$$G_t = \sum_{i \in U} p^i G_t^i = \sum_{i \in U} p^i \nabla \mathcal{L}^i(w_t^i) \quad (12)$$

as the full gradient of the population at time  $t$ . Meanwhile, denote

$$g_t^i = \frac{1}{m^i} \sum_{j \in S^{i,*}} \delta_j^{i,*} \nabla \mathcal{L}_j^i(w_t^i), \quad (13)$$

where  $(\delta^{i,*}, S^{i,*})$  is defined in Eq.(5), as the gradient computed from the coreset of client  $i$  at time  $t$ . And denote  $g_t = \sum_{i \in U} p^i g_t^i$  as the population coreset gradient at time  $t$ .

In practice, within one round, only a subset of  $K$  randomly selected clients will update their parameters, and the choices of clients vary each round. In order to facilitate the analysis under the random selection scheme, the following thought trick is introduced to circumvent the difficulty: we assume that FedCore always activates **all** devices at the beginning of each round, while only aggregates parameters from those sampled devices at the end of one round. It is clear that this updating scheme is equivalent to the original. More specifically, the updating scheme in FedCore is given by,  $\forall i \in U$ ,

$$\begin{aligned} v_{t+1}^i &= w_t^i - \eta_t g_t^i, \\ w_{t+1}^i &= \begin{cases} v_{t+1}^i & \text{if } t+1 \notin \mathcal{I}_E, \\ \frac{1}{K} \sum_{k \in U_t} v_{t+1}^k & \text{if } t+1 \in \mathcal{I}_E, \end{cases} \end{aligned} \quad (14)$$

where  $\mathcal{I}_E = \{rE \mid r = 1, 2, \dots, R\}$  is the set of global synchronization steps, and  $U_t$  is the set of  $K$  selected clients at time  $t$ . An additional variable  $v_{t+1}^i$  is introduced to represent the immediate result of one step GD update from  $w_t^i$ , and  $w_t^i$  is the final model parameters maintained by client  $i$  at time  $t$ , (possibly after the global synchronization).

In addition, two virtual sequences are introduced in the subsequent analysis to denote the population-averaged model parameters, following the ideas from [15, 30, 50]:

$$\bar{v}_t = \sum_{i \in U} p^i v_t^i, \text{ and } \bar{w}_t = \sum_{i \in U} p^i w_t^i, \quad (15)$$

where  $\bar{v}_{t+1}$  results from an single GD step of from  $\bar{w}_t$ :

$$\bar{v}_{t+1} = \bar{w}_t - \eta_t g_t. \quad (16)$$

## A.2 Assumptions and Convergence Results

The following are the detailed assumptions required for the convergence analysis.

**Assumption A.1 ( $L$ -smoothness)**  $\forall i \in U, \mathcal{L}^i$  is  $L$ -smooth: for all  $v, w \in \mathcal{W}$ ,

$$\mathcal{L}^i(v) \leq \mathcal{L}^i(w) + (v - w)^\top \nabla \mathcal{L}^i(w) + \frac{L}{2} \|v - w\|_2^2.$$

**Assumption A.2 ( $\mu$ -strong convexity)**  $\forall i \in U, \mathcal{L}^i$  is  $\mu$ -strongly convex: for all  $v, w \in \mathcal{W}$ ,

$$\mathcal{L}^i(v) \geq \mathcal{L}^i(w) + (v - w)^\top \nabla \mathcal{L}^i(w) + \frac{\mu}{2} \|v - w\|_2^2.$$

**Assumption A.3 ( $\epsilon$ -coreset)** For any client  $i$  and time step  $t$ , with probability one, the coreset gradient  $g_t^i$  in Eq.(13) is an  $\epsilon$ -approximation to the full-set gradient  $G_t^i$  in Eq.(11):

$$\|g_t^i - G_t^i\| \leq \epsilon, \quad \forall i \in U, \text{ and } t \in \{0, 1, \dots, ER\}, \quad \text{with probability one.}$$

**Assumption A.4 ( $D$ -bounded gradient)** For any client  $i$  and time step  $t$ , with probability one, 2-norms of the coreset gradient  $g_t^i$  in Eq.(13) and the full-set gradient  $G_t^i$  in Eq.(11) are uniformly upper bounded by a constant  $D > 0$ :

$$\max \{\|g_t^i\|, \|G_t^i\|\} \leq D, \quad \forall i \in U, \text{ and } t \in \{0, 1, \dots, ER\}, \quad \text{with probability one.}$$

**Assumption A.5 ( $\Gamma$ -heterogeneity)** Let  $\mathcal{L}_*$  and  $\mathcal{L}_*^i$  be the minimum values of  $\mathcal{L}$  and  $\mathcal{L}^i$ , respectively. Assume there is a positive constant  $\Gamma > 0$  such that  $\Gamma \geq \mathcal{L}_* - \sum_{i \in U} p^i \mathcal{L}_*^i$ .

**Assumption A.6 (Random sampling)** For any time step  $t$ , assume  $U_t$  contains a subset of  $K$  indices randomly selected with replacement according to the sampling probabilities  $\{p^i\}_{i \in U}$ .

**Comments on Assumptions** Assumption A.1 and A.2 are standard assumptions in convex optimization [6]; typical examples are linear/ridge regression, logistic regression, and regularized support vector machines. Assumption A.3 characterizes the approximation capability of the coreset to the full-set, which is standard in the theoretical works on coreset-based gradient descent methods [37, 44]. Assumption A.4 on the bounded gradient is a widely adopted setting in the existing theoretical works for federated learning and coreset methods [28, 30, 37]. Meanwhile, note that Assumptions A.3 and A.4 are presented in a probabilistic form to account for the potential randomness resulting from the coreset construction steps in FedCore. Assumption A.5 quantifies the degree of heterogeneity among different clients. In the special case when data from all the clients are i.i.d., then  $\mathcal{L}_* - \sum_{i \in U} p^i \mathcal{L}_*^i \rightarrow 0$  as the number of samples grows. Assumption A.6 assumes the  $K$  clients are selected from the distribution  $\{p^i\}_{i \in U}$  independently and with replacement, which is a common set-up in both theoretical and empirical works [28, 30].

**Randomness in FedCore** Note that randomness in FedCore can be attributed to three sources: client selection, coreset construction and model initialization  $w_0$ . Throughout the subsequent analysis and statements, unless otherwise specified, the expectation  $\mathbb{E}[\cdot]$  is taken over all three sources of randomness. Meanwhile, the notation  $\mathbb{E}_{U_t}[\cdot]$  is also introduced to denote the expectation over the random client selection at time  $t$ , conditioned on the other sources of randomness.

### A.3 Proofs of Main Results

The convergence of FedCore is established by the following theorem, which can be considered as a more detailed version of Theorem 5.1.

**Theorem A.7** *Assume Assumptions A.1, A.2, A.3, A.4, A.5, A.6 hold with constants  $L, \mu, \epsilon, D, \Gamma$ . Consider FedCore with  $R$  rounds and each round contains  $E$  epochs. For  $t \in \{0, 1, \dots, ER\}$ , set the learning rate*

$$\eta_t = \frac{\alpha}{t + \beta}, \quad \text{with } \alpha = \frac{2}{\mu} \text{ and } \beta = \max \left\{ E, \frac{8L}{\mu} \right\}.$$

*The model  $w_{out}$  output by FedCore after  $R$  rounds of training satisfies*

$$\mathbb{E} [\|w_{out} - w_*\|^2] \leq A_1 + \frac{A_2}{ER + \beta}, \quad (17)$$

*where the constants  $A_1$  and  $A_2$  are given by:*

$$\begin{aligned} A_1 &= \frac{2\epsilon D}{\mu^2}, \\ A_2 &= \max \left\{ \beta \mathbb{E} [\|w_0 - w_*\|^2], \frac{4}{\mu^2} \left[ \frac{4E^2 D^2}{K} + 8(E-1)^2 D^2 + 6L\Gamma + \epsilon^2 + 2\epsilon D \right] \right\}. \end{aligned} \quad (18)$$

*Here  $w_* = \operatorname{argmin}_{w \in \mathcal{W}} \mathcal{L}(w)$  as defined in Eq.(7) and the expectation is taken over the randomness in client selection, coreset construction and model initialization  $w_0$ . Consequently,*

$$\mathbb{E} [\mathcal{L}(w_{out}) - \mathcal{L}(w_*)] \leq \frac{L}{2} \left( A_1 + \frac{A_2}{ER + \beta} \right). \quad (19)$$

The proof of Theorem A.7 is based on the following three key lemmas, whose proofs are deferred to appendix A.3.

**Lemma A.8** *Under the setting of Theorem A.7, for  $t + 1 \in \mathcal{I}_E = \{rE \mid r = 1, 2, \dots, R\}$ , the set of global synchronization steps,*

$$\mathbb{E}_{U_t} [\bar{w}_{t+1}] = \bar{v}_{t+1}. \quad (20)$$

**Lemma A.9** *Under the setting of Theorem A.7, for  $t + 1 \in \mathcal{I}_E = \{rE \mid r = 1, 2, \dots, R\}$ , the set of global synchronization steps, the expected difference between  $\bar{v}_{t+1}$  and  $\bar{w}_{t+1}$  is bounded by*

$$\mathbb{E}_{U_t} [\|\bar{v}_{t+1} - \bar{w}_{t+1}\|^2] \leq \frac{4}{K} \eta_t^2 E^2 D^2. \quad (21)$$

**Lemma A.10** Under the setting of Theorem A.7, for any time step  $t + 1 \in \{1, 2, \dots, ER\}$ ,

$$\mathbb{E} \left[ \|\bar{v}_{t+1} - w_*\|^2 \right] \leq (1 - \eta_t \mu) \mathbb{E} \left[ \|\bar{w}_t - w_*\|^2 \right] + \eta_t \cdot A_3 + \eta_t^2 \cdot A_4, \quad (22)$$

where

$$A_3 = \frac{2\epsilon D}{\mu}, \quad A_4 = 8(E - 1)^2 D^2 + 6L\Gamma + \epsilon^2 + 2\epsilon D. \quad (23)$$

**Proof of Theorem A.7** First note the following decomposition:

$$\begin{aligned} \|\bar{w}_{t+1} - w_*\|^2 &= \|\bar{w}_{t+1} - \bar{v}_{t+1} + \bar{v}_{t+1} - w_*\|^2 \\ &= \underbrace{\|\bar{w}_{t+1} - \bar{v}_{t+1}\|^2}_{H_1} + 2 \underbrace{\langle \bar{w}_{t+1} - \bar{v}_{t+1}, \bar{v}_{t+1} - w_* \rangle}_{H_2} + \underbrace{\|\bar{v}_{t+1} - w_*\|^2}_{H_3}. \end{aligned} \quad (24)$$

For the first term  $H_1$  in Eq.(24), note that when  $t + 1 \notin \mathcal{I}_E$ , we have  $\bar{v}_{t+1} = \bar{w}_{t+1}$ , and  $H_1$  vanishes. Additionally, if  $t + 1 \in \mathcal{I}_E$ , then the expectation of  $H_1$  is bounded by Lemma A.9:

For the second term  $H_2$  in Eq.(24), when  $t + 1 \notin \mathcal{I}_E$ ,  $H_2$  vanishes since  $\bar{v}_{t+1} = \bar{w}_{t+1}$ . Additionally, when  $t + 1 \in \mathcal{I}_E$ ,  $H_2$  vanishes under the expectation  $\mathbb{E}_{U_t}[\cdot]$ , due to the unbiasedness of  $\bar{w}_{t+1}$  stated in Lemma A.8.

For the third term  $H_3$  in Eq.(24), its expectation is bounded by Lemma A.10 for any time step  $t + 1 \in \{1, 2, \dots, ER\}$ .

Overall, combining the bounds on  $H_1$ ,  $H_2$  and  $H_3$  together, we have for any  $t + 1 \in \{1, 2, \dots, ER\}$ ,

$$\mathbb{E} \left[ \|\bar{w}_{t+1} - w_*\|^2 \right] \leq (1 - \eta_t \mu) \mathbb{E} \left[ \|\bar{w}_t - w_*\|^2 \right] + \eta_t \cdot A_3 + \eta_t^2 \cdot \left( \frac{4E^2 D^2}{K} + A_4 \right), \quad (25)$$

where  $A_3, A_4$  are defined in Eq.(23). For simplicity, denote

$$A_5 := \frac{4E^2 D^2}{K} + A_4. \quad (26)$$

Now we will prove by induction that under the diminishing step size  $\eta_t = \frac{\alpha}{t+\beta}$  with  $\alpha = \frac{2}{\mu}$  and  $\beta = \max \left\{ E, \frac{8L}{\mu} \right\}$ , for any time step  $t \in \{0, 1, \dots, ER\}$ ,

$$\mathbb{E} \left[ \|\bar{w}_t - w_*\|^2 \right] \leq A_1 + \frac{A_2}{t + \beta}, \quad (27)$$

where  $A_1, A_2$  are defined in Eq.(18).

First, note that the definition of  $A_2$  in Eq.(18) ensures that Eq.(27) holds for  $t = 0$ . Assume Eq.(27) holds for some time step  $t$ . Then for time step  $t + 1$ , by Eq.(25), we have

$$\begin{aligned} \mathbb{E} \left[ \|\bar{w}_{t+1} - w_*\|^2 \right] &\leq \left( 1 - \frac{\alpha \mu}{t + \beta} \right) \cdot \left( A_1 + \frac{A_2}{t + \beta} \right) + \frac{\alpha}{t + \beta} \cdot A_3 + \left( \frac{\alpha}{t + \beta} \right)^2 \cdot A_5, \\ &= A_1 + \left( 1 - \frac{\alpha \mu}{t + \beta} \right) \cdot \frac{A_2}{t + \beta} + \left( \frac{\alpha}{t + \beta} \right)^2 \cdot A_5 + \frac{\alpha(A_3 - \mu A_1)}{t + \beta} \end{aligned} \quad (28)$$

Note that by the definitions of  $A_1$  in Eq.(18) and  $A_3$  in Eq.(23),

$$A_3 = \mu A_1. \quad (29)$$

Meanwhile,

$$\begin{aligned} \left( 1 - \frac{\alpha \mu}{t + \beta} \right) \cdot \frac{A_2}{t + \beta} + \left( \frac{\alpha}{t + \beta} \right)^2 \cdot A_5 &= \frac{(t + \beta - 1)A_2}{(t + \beta)^2} + \left[ \frac{\alpha^2 A_5}{(t + \beta)^2} - \frac{(\alpha \mu - 1)A_2}{(t + \beta)^2} \right] \\ &\leq \frac{A_2}{t + \beta + 1} + \left[ \frac{\alpha^2 A_5}{(t + \beta)^2} - \frac{(\alpha \mu - 1)A_2}{(t + \beta)^2} \right] \\ &= \frac{A_2}{t + \beta + 1} + \frac{1}{(t + \beta)^2} \left[ \frac{4A_5}{\mu^2} - A_2 \right] \\ &\leq \frac{A_2}{t + \beta + 1}. \end{aligned} \quad (30)$$



Here the second equality in Eq.(30) is due to the fact that  $\alpha = \frac{2}{\mu}$ , and the second inequality in Eq.(30) comes from the fact that  $A_2 \geq \frac{4A_5}{\mu^2}$ , which is a direct consequence of the definitions of  $A_2$  in Eq.(18) and  $A_5$  in Eq.(26).

Plugging Eq.(29) and Eq.(30) into Eq.(28) completes the proof of the induction hypothesis in Eq.(27). Specifically, the model  $w_{\text{out}} = \bar{w}_{ER}$  output by FedCore after  $R$  rounds satisfies Eq.(17).

Furthermore, by the  $L$ -smoothness of  $\mathcal{L}$  (Assumption A.1),

$$\mathbb{E} [\mathcal{L}(w_{\text{out}}) - \mathcal{L}(w_*)] \leq \frac{L}{2} \cdot \mathbb{E} [\|w_{\text{out}} - w_*\|^2] \leq \frac{L}{2} \left( A_1 + \frac{A_2}{ER + \beta} \right). \quad (31)$$

□

#### A.4 Proofs of Lemmas

**Proof of Lemma A.8** This lemma is a direct consequence of Assumption A.6. More specifically, for  $t + 1 \in \mathcal{I}_E = \{rE \mid r = 1, 2, \dots, R\}$ ,

$$\mathbb{E}_{U_t} [\bar{w}_{t+1}] = \mathbb{E}_{U_t} \left[ \frac{1}{K} \sum_{k \in U_t} v_{t+1}^k \right] = \frac{1}{K} \cdot K \cdot \mathbb{E}_{k \in U_t} [v_{t+1}^k] = \sum_{i \in U} p^i v_{t+1}^i = \bar{v}_{t+1},$$

where the second equality comes from the linearity of expectation, and the third equality is due to Assumption A.6. □

**Proof of Lemma A.9** Lemma A.9 is a direct consequence of Lemma 5 in [30]. The proof is outlined as follows.

For  $t + 1 \in \mathcal{I}_E = \{rE \mid r = 1, 2, \dots, R\}$ ,  $\bar{w}_{t+1} = \frac{1}{K} \sum_{k \in U_t} v_{t+1}^k$ . Taking expectation over  $U_t$ ,

$$\begin{aligned} \mathbb{E}_{U_t} [\|\bar{w}_{t+1} - \bar{v}_{t+1}\|^2] &= \mathbb{E}_{U_t} \left[ \frac{1}{K^2} \sum_{k \in U_t} \|v_{t+1}^k - \bar{v}_{t+1}\|^2 \right] = \frac{1}{K} \mathbb{E}_{k \in U_t} [\|v_{t+1}^k - \bar{v}_{t+1}\|^2] \\ &= \frac{1}{K} \sum_{i \in U} p^i \|v_{t+1}^i - \bar{v}_{t+1}\|^2 \end{aligned} \quad (32)$$

where the first equality follows from Assumption A.6 that  $\{v_{t+1}^k\}_{k \in U_t}$  are independent and unbiased with  $\mathbb{E}_{k \in U_t} [v_{t+1}^k] = \bar{v}_{t+1}$ .

To bound Eq.(32), first note that since  $t + 1 \in \mathcal{I}_E$ ,  $t_0 := t + 1 - E \in \mathcal{I}_E$  is also a synchronization time, which implies  $\{w_{t_0}^i\}_{i \in U}$  is identical. Then,

$$\begin{aligned} \sum_{i \in U} p^i \|v_{t+1}^i - \bar{v}_{t+1}\|^2 &= \sum_{i \in U} p^i \|(v_{t+1}^i - \bar{w}_{t_0}) - (\bar{v}_{t+1} - \bar{w}_{t_0})\|^2 \\ &= \left( \sum_{i \in U} p^i \|v_{t+1}^i - \bar{w}_{t_0}\|^2 \right) - \|\bar{v}_{t+1} - \bar{w}_{t_0}\|^2 \leq \sum_{i \in U} p^i \|v_{t+1}^i - \bar{w}_{t_0}\|^2, \end{aligned} \quad (33)$$

where the second equality results from  $\sum_{i \in U} p^i (v_{t+1}^i - \bar{w}_{t_0}) = \bar{v}_{t+1} - \bar{w}_{t_0}$ . Combining Eq.(32) and Eq.(33), we have

$$\begin{aligned} \mathbb{E}_{U_t} [\|\bar{w}_{t+1} - \bar{v}_{t+1}\|^2] &\leq \frac{1}{K} \sum_{i \in U} p^i \|v_{t+1}^i - \bar{w}_{t_0}\|^2 = \frac{1}{K} \sum_{i \in U} p^i \|v_{t+1}^i - w_{t_0}^i\|^2 \\ &= \frac{1}{K} \sum_{i \in U} p^i \left\| \sum_{\tau=t_0}^t \eta_\tau g_\tau^i \right\|^2 \leq \frac{1}{K} \sum_{i \in U} p^i E \sum_{\tau=t_0}^t \|\eta_\tau g_\tau^i\|^2 \\ &\leq \frac{1}{K} E \sum_{\tau=t_0}^t \eta_\tau^2 D^2 \leq \frac{1}{K} E^2 \eta_{t_0}^2 D^2 \leq \frac{4}{K} \eta_t^2 E^2 D^2. \end{aligned} \quad (34)$$

Here, the second inequality in Eq. (34) follows from the Cauchy-Schwarz inequality. The third inequality is a result of Assumption A.4. The fourth inequality is justified by the fact that  $\eta_t = \frac{\alpha}{t+\beta}$  is non-increasing. Lastly, the last inequality holds since, by definition,  $\beta = \max\left\{E, \frac{8L}{\mu}\right\} \geq E$ , and therefore  $\eta_{t_0} \leq 2\eta_{t_0+E-1}$ .  $\square$

**Proof of Lemma A.10** First, by Eq.(16), we have

$$\|\bar{v}_{t+1} - w_*\|^2 = \|\bar{w}_t - w_* - \eta_t g_t\|^2 = \|\bar{w}_t - w_*\|^2 + \underbrace{\eta_t^2 \|g_t\|^2}_{F_1} - \underbrace{2\eta_t \langle \bar{w}_t - w_*, g_t \rangle}_{F_2} \quad (35)$$

To bound  $F_1$  in Eq.(35), note that

$$\begin{aligned} F_1 &= \eta_t^2 \|g_t\|^2 = \eta_t^2 \left\| \sum_{i \in U} p^i g_t^i \right\|^2 \leq \eta_t^2 \sum_{i \in U} p^i \|g_t^i\|^2 = \eta_t^2 \sum_{i \in U} p^i \|G_t^i + g_t^i - G_t^i\|^2 \\ &= \eta_t^2 \left( \sum_{i \in U} p^i \|G_t^i - g_t^i\|^2 + 2 \sum_{i \in U} p^i \langle G_t^i, g_t^i - G_t^i \rangle + \sum_{i \in U} p^i \|G_t^i\|^2 \right) \\ &= \eta_t^2 \left( \sum_{i \in U} p^i \|G_t^i - g_t^i\|^2 + 2 \sum_{i \in U} p^i \|G_t^i\| \|g_t^i - G_t^i\| + \sum_{i \in U} p^i \|G_t^i\|^2 \right) \\ &\leq \eta_t^2 \left( \epsilon^2 + 2\epsilon D + \sum_{i \in U} p^i \|G_t^i\|^2 \right) \\ &\leq \eta_t^2 \left( \epsilon^2 + 2\epsilon D + 2L \sum_{i \in U} p^i (\mathcal{L}^i(w_t^i) - \mathcal{L}_*^i) \right). \end{aligned} \quad (36)$$

Here the first inequality in Eq.(36) is due to the convexity of  $\|\cdot\|^2$ . The second inequality comes from Assumption A.4 and Assumption A.3. The last inequality follows from the fact that for  $L$ -smooth  $\mathcal{L}^i$  (Assumption A.1),

$$\|G_t^i\|^2 \leq 2L (\mathcal{L}^i(w_t^i) - \mathcal{L}_*^i). \quad (37)$$

To bound  $F_2$  in Eq.(35), note that

$$\begin{aligned} F_2 &= -2\eta_t \langle \bar{w}_t - w_*, g_t \rangle = -2\eta_t \sum_{i \in U} p^i \langle \bar{w}_t - w_*, g_t^i \rangle \\ &= -2\eta_t \sum_{i \in U} p^i \langle \bar{w}_t - w_t^i, G_t^i \rangle - 2\eta_t \sum_{i \in U} p^i \langle w_t^i - w_*, G_t^i \rangle + 2\eta_t \sum_{i \in U} p^i \langle \bar{w}_t - w_*, G_t^i - g_t^i \rangle \\ &\leq -2\eta_t \sum_{i \in U} p^i \langle \bar{w}_t - w_t^i, G_t^i \rangle - 2\eta_t \sum_{i \in U} p^i \langle w_t^i - w_*, G_t^i \rangle + 2\eta_t \epsilon \cdot \|\bar{w}_t - w_*\| \end{aligned} \quad (38)$$

Here the last inequality in Eq.(38) is due to the Cauchy-Schwarz inequality and Assumption A.3. Moreover, by the Cauchy-Schwarz inequality and the AM-GM inequality,

$$-2 \langle \bar{w}_t - w_t^i, G_t^i \rangle \leq \frac{1}{\eta_t} \|\bar{w}_t - w_t^i\|^2 + \eta_t \|G_t^i\|^2 \leq \frac{1}{\eta_t} \|\bar{w}_t - w_t^i\|^2 + 2L\eta_t (\mathcal{L}^i(w_t^i) - \mathcal{L}_*^i), \quad (39)$$

where the last inequality in Eq.(39) follows from Eq.(37). In addition, by the  $\mu$ -strong convexity of  $\mathcal{L}^i$ , Assumption A.2,

$$-2 \langle w_t^i - w_*, G_t^i \rangle \leq -(\mathcal{L}^i(w_t^i) - \mathcal{L}^i(w_*)) - \frac{\mu}{2} \|w_t^i - w_*\|^2. \quad (40)$$

The  $\mu$ -strong convexity of  $\mathcal{L}$ , together with the optimality of  $w_*$ , also implies that

$$\|\bar{w}_t - w_*\| \leq \frac{1}{\mu} \|\nabla \mathcal{L}(\bar{w}_t) - \nabla \mathcal{L}(w_*)\| = \frac{1}{\mu} \|\nabla \mathcal{L}(\bar{w}_t)\| \leq \frac{D}{\mu}, \quad (41)$$

where the last inequality comes from Assumption A.4.

Now combining Eq.(35) with Eq.(36), Eq.(38), Eq.(39), Eq.(40), and Eq.(41), it follows that

$$\begin{aligned}
\|\bar{v}_{t+1} - w_*\|^2 &\leq \underbrace{\|\bar{w}_t - w_*\|^2 - \eta_t \mu \sum_{i \in U} p^i \|w_t^i - w_*\|^2}_{F_3} + \sum_{i \in U} p^i \|\bar{w}_t - w_t^i\|^2 \\
&\quad + \underbrace{4L\eta_t^2 \sum_{i \in U} p^i (\mathcal{L}^i(w_t^i) - \mathcal{L}^i(w_*)) - 2\eta_t \sum_{i \in U} p^i (\mathcal{L}^i(w_t^i) - \mathcal{L}^i(w_*))}_{F_4} \\
&\quad + \eta_t \cdot \frac{2\epsilon D}{\mu} + \eta_t^2 \cdot (\epsilon^2 + 2\epsilon D)
\end{aligned} \tag{42}$$

To bound  $F_3$  in Eq.(42), it follows by the convexity of  $\|\cdot\|^2$  that

$$F_3 \leq \|\bar{w}_t - w_*\|^2 - \eta_t \mu \left\| \sum_{i \in U} p^i (w_t^i - w_*) \right\|^2 = (1 - \eta_t \mu) \|\bar{w}_t - w_*\|^2. \tag{43}$$

Meanwhile, it is shown by Lemma 1 of [30] that  $F_4$  in Eq.(42) is bounded by

$$F_4 \leq \eta_t^2 \cdot 6L\Gamma + \sum_{i \in U} p^i \|\bar{w}_t - w_t^i\|^2. \tag{44}$$

By combining Eq.(42) with Eq.(43) and Eq.(44), it follows that

$$\begin{aligned}
\|\bar{v}_{t+1} - w_*\|^2 &\leq (1 - \eta_t \mu) \|\bar{w}_t - w_*\|^2 + \eta_t \cdot \frac{2\epsilon D}{\mu} + \eta_t^2 \cdot (6L\Gamma + \epsilon^2 + 2\epsilon D) \\
&\quad + 2 \underbrace{\sum_{i \in U} p^i \|\bar{w}_t - w_t^i\|^2}_{F_5}.
\end{aligned} \tag{45}$$

Finally, to bound  $F_5$  in Eq.(45), one can apply the same argument used in bounding Eq.(32). More specifically, for any  $t$ , there exists a  $t_0 \leq t$  such that  $t - t_0 \leq E - 1$  and  $w_{t_0}^i = \bar{w}_{t_0}$  for all  $i \in U$ . Then, by following the same arguments as in Eq.(33) and Eq.(34), it is easy to verify that:

$$F_5 \leq \eta_t^2 \cdot 4(E - 1)^2 D^2. \tag{46}$$

By plugging Eq.(46) into Eq.(45), we complete the proof of Lemma A.10.  $\square$

## B Evaluation Details and Extra Results

### B.1 Experimental Hardware and Hyper-parameters

In our evaluations, we utilize a physical server equipped with an Intel Core X Series Core i9 10920X CPU [19] and a NVIDIA GeForce RTX 2080 Ti GPU [41]. The server runs on the Linux Ubuntu 20.04 operating system. The hyper-parameters used in our evaluations are detailed in Table 3.

**Table 3:** Hyper-parameters

Hyper-parameters	MNIST	Shakespeare	Synthetic
Optimizer	SGD	SGD	SGD
Learning Rate	0.03	0.03	0.001
Batch Size	8	8	8
Local Epoch	10	10	10
Communication Round	100	30	100
Number of Clients	1000	143	30
Number of Clients per Round	100	10	10
$\mu$ in FedProx	0.1	0.001	0.1

### B.2 Extra Evaluation Results

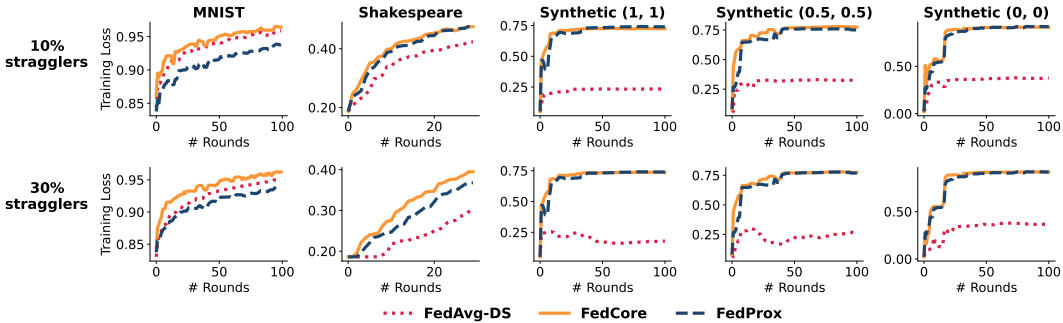


**Figure 6:** The test accuracy curves for FedAvg-DS, FedCore, and FedProx at 10% and 30% stragglers.

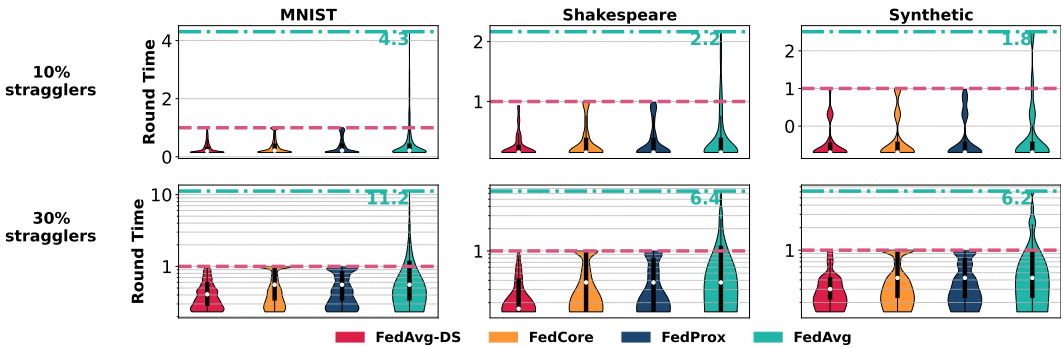


**Figure 7:** Round duration distribution across all clients, training rounds, and three benchmarks at 10% and 30% straggler settings, utilizing a log-scale y-axis for better visualization of the 30% straggler scenario.